Modelling Magnetic Drug Delivery with Differential Equations

Delice Mambi-Lambu (30077966)

November 14, 2022

Abstract

The report is about finding the most mathematically accurate way to model the process of magnetic drug delivery with differential equations. Throughout the project, we will consider several aspects of magnetic drug delivery. For example, the fluid flow, the shape of the magnetic nanoparticle (MNP), the trajectories of the MNPs, and the geometry of the channel travelled. Then, we justified the choices and assumptions taken to deal with this model. We see several aspects of magnetic drug delivery that need to be treated delicately and with the resources provided. The project results show that with a clear channel, a large number of particles will hit the boundary of a blood vessel (as expected), and the number of forces applied to the particle will influence the number of particles that will hit the boundary of the blood vessel. Furthermore, we will consider the limitations of the models as we will seek to discern if the models are a mathematically accurate representation of magnetic drug delivery.

Keywords: Magnetic Drug Targeting, Mathematical Model, Poiseuille Flow, Stokes Law, Magnetic Field

1 Introduction

We define Drug Targeting as the process of delivering drugs to a specific part of the body exclusively. Targets can range from organs (such as the kidney or liver) to any receptors. There are two approaches to drug delivery. One method is to let a person take a drug and let the drug enter the body's circulation system hoping that it will eventually reach the target tissue by a large proportion and the drug will be able to carry out its purpose successfully. We find that many drug particles through this method did not reach the target site. The majority of carrier particles of the drug will be excreted out of the circulation system via the liver/spleen/kidney/bone marrow/lungs (The set of organs known as RES organs) [10]. The drug's effectiveness decreases the higher the dosage [6].

So, there is a need for drug delivery to be as efficient and effective as possible. Hence, the development of the use of magnetic fields in drug transportation. Magnetic Drug Targeting is the delivery of a therapeutic agent to the desired target area by using a magnetic field.

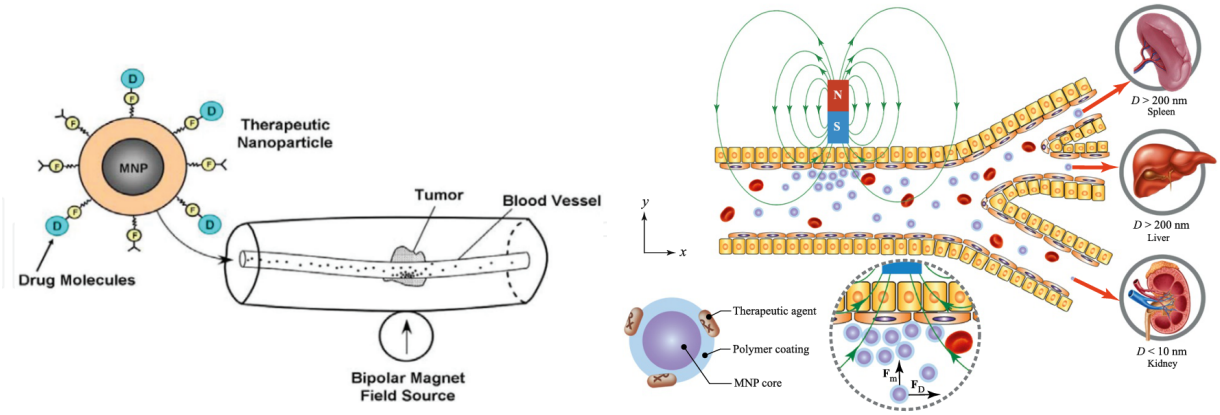

Figure 1: Two diagrams representing the process a Magnetic Nano Particle undergoes to target a tumour and how the size of the carrier particle can affect the path taken. [10]

We use a magnetic field because magnetic fields are harmless to our biological systems and are adaptable to any part of the body. The design of the carrier particle involves having a magnetic nanoparticle coated with biocompatible hydrophilic polymer chains (i.e. PEG, PEO, SiO_2) [10]. Then the biocompatible coating can be used by attaching Carboxyl groups, Biotin, Avidin, and amino groups. These act as attachment points for coupling cytotoxic drugs or target antibodies.

The drug is injected into the bloodstream and directed and stopped by the magnetic field in the target area. The process is very effective and efficient in delivering drugs to a disease location. Hence, very high concentrations of chemotherapeutic or radiological agents will reach the target site (for example, a tumour).[1] Therefore, a higher success rate of effectiveness of the drug in comparison to systemic drug delivery.

The advantages of this approach are that it minimises side effect risk. The system reduces the circulating concentration of free drugs by 100 or more, and there is a decline in regular cell tissue damage rate.[6] However, the system is expensive to carry out. The drug cannot be targeted to some locations in the organs. There are limitations to the magnets used as the gradients must be constant to avoid overdosing on a drug in a localised area. [10] Furthermore, we now seek ways to represent this problem in the mathematical sense as we look to study the trajectories and the paths the carrier particle takes to reach the target.

2 Methodology

This section is a summary from sources [9] and [4]

The project takes numerical and analytical approaches to provide solutions to the models and aspects of the models. As for the Numerical Approach, we use the implicit Runge-Kutta method in the fourth order (RK4). Whereas, in analytics, we use the process of non-dimensionalisation, phase plane method and multiple integral to provide solutions. In

this section we focus on the implicit Runge-Kutta method in the fourth order (RK4) and phase plane method.

2.1 Numerical Methods

The Runge-Kutta method was implemented using `solve_ivp` from Python's SciPy Library and was used to solve the differential equations for modelling magnetic drug delivery with diffrential equations.

2.1.1 Runge-Kutta Method

The implicit Runge-Kutta method used in this model is the fourth-order (RK4) method. An increment of y is estimated using a weighted average, $k_{1\text{-}4}$. They are defined as follows and from the initial step the next two iterations simply evaluates the Euler Approximation []

$$k_1 = f(x_n, y_n) \qquad k_2 = f(x_n + \frac{1}{2}h, y_n + \frac{1}{2}k_1) \qquad k_3 = f(x_n + \frac{1}{2}h, y_n + \frac{1}{2}k_2) \tag{1}$$

These two calculate the value of x at the midpoint of the interval and therefore gives a prediction of the gradient at the prior k.

$$k_4 = f(x_n + h, y_n + k_3) \tag{2}$$

k_4 computes the final point of the interval at the right side of k_3. These weights form the algorithm:

$$y_{n+1} = y_n + \frac{1}{6}(K_1 + 2K_2 + 2K_3 + K_4) \tag{3}$$

The Runge-Kutta method realises an increase in accuracy to the Euler method by incorporating the trapezoidal rule formula. As seen in 3, k_2 and k_3 are weighted twice as much as k_1 and k_4. In combination with this, $k_{1\text{-}4}$ accounts for the whole width of the interval; this makes the algorithm symetric. The local error for this method is ($\mathcal{O}$ (h^5)) and global error is ($\mathcal{O}$ (h^4)).

2.1.2 Numerical Methods to Study Fractional Capture

Now we look to use numerical methods to calculate the number of particles hit the target region. We measure it by calculating the fraction of capture α defined as the ratio between the number of particles that converge towards the target wall between $0 \leq x \leq L$ where L represents the Length of the magnet and, the number of particles entering the vessel from x between $0 < y < h$ where y represents the height of the vessel.

2.2 Analytical Methods

2.2.1 The Phase Plane Method

The project uses the phase plane method by applying it to a non-linear autonomous differential equations system - where our system does not explicitly depend on the independent

variable (In this case, t). Here we have that we cannot solve the system by using standard techniques to produce a solution that is in closed form. We can express the system in the following form

$$du/dt = f(u,v) \qquad dv/dt = g(u,v) \tag{4}$$

Where u and v are variables dependent on t. We now seek to study the local behaviour of the solutions at points that satisfy the system of equations. Beginning with the study of trajectories on the u-v plane - the gradient is defined as $dv/du = g(u,v)/f(u,v)$. We define the *null clines* as the set of curves where $dv/du = 0$ or $dv/du = \infty$. The nullclines split the u-v plane into regions where du/dt and dv/dt are either positive or negative. The critical points of the u-v plane are defined as the points where du/dt and dv/dt equate to zero. We say that the critical points are only stable steady solutions to $f(u,v) = 0$ and $g(u,v) = 0$ if the localised trajectories converge to the point, otherwise we say that they are unstable solutions. To characterise the critical points, we linearise $f(u,v)$ and $g(u,v)$ about the critical points (v_c, u_c) and then perform a Taylor series expansion to first order such that we are left with a constant coefficient system of linear ODEs, with eigenvector solutions of the form

$$(U,V)^T = A(\alpha_1 + \beta_1)^T e^{\lambda_1 t} + B(\alpha_2 + \beta_2)^T e^{\lambda_2 t} = C(dU/dt, dV/dt)^T \tag{5}$$

The eigenvalues λ_1 and λ_2 therefore determine the solution behaviour near the critical point. Where $\lambda_1, \lambda_2 \in \mathbb{R}$ $\lambda_1 \leq \lambda_2 < 0$ the critical point is a Stable Node. $\lambda_1 > 0 > \lambda_2$ the critical point is a Unstable Saddle Point and $\lambda_1 \geq \lambda_2 > 0$ Is an Unstable Node. In the case where $\lambda \in \mathbb{C}$ where $\lambda = p + \boldsymbol{i}q$. If $\mathbb{R}(\lambda) < 0$ we have a Stable Spiral. $\mathbb{R}(\lambda) = 0$ we have a Centre and, $\mathbb{R}(\lambda) > 0$ we have a Unstable Spiral. Where $\lambda_1\lambda_2 = 0$ there is not enough information to determine the stability and therefore we must use other techniques to learn about the localised behaviour around the saddle point.

Before producing a rough plot of the analytic solution in the $u-v$ plane, We must determine the symmetry of the solution about the u axis. The process can be simplfied if $g(u,v)$ and $f(u,v)$ are invariant under the transforms $v \to -v$, $u \to -u$ and $t \to -t$, because then the solution trajectories have reflectional symmetry across the u axis, and the phase trajectories are also closed crossing $u = 0$. In the case that the functions are not invariant under these transforms, then one must repeat the phase-plane procedure with the new system to determine the global behaviour of the solution.

3 Considerations and Assumptions

We now consider the aspects that occur during the process of Drug Delivery of MNPs. We have an MNP injected into the bloodstream that flows until it is stopped by a magnetic field at the target site (if reached). The first thing to consider is the shape of the particle. In figure 1 we see that our MNP has a spiked-spherical shape. In this model, we will disregard the spikes and assume that the carrier particle will be in the shape of a sphere; this is important as it enables us to use Stokes Law for Drag to simplify calculations. Secondly, we assume that the blood behaves like a Newtonian, incompressible fluid and the fluid flow is laminar.

In this project, we will also assume that the flow in the vessel is Poiseuille flow. However, the model breaks down where the diameter of the vessel is below $10\mu m$. [3] Furthermore, We assume that no friction acts between the fluid and the particle. We also consider that the vessel is clear of any foreign particles. Hence, we only consider in the blood vessel the blood fluid itself and the carrier particle, limiting the number of interactions between the carrier particle and other foreign objects such as Red Blood Cells, Fatty Deposits, and More. Also, we consider the geometry of the shape of the vessel. In this project, we assume that the vessel is shaped as a perfect cylinder. Furthermore, we assume that no other inertial forces act on the particle. Lastly, we consider the magnetic force to be a constant, and we will apply this in only one direction.

4 The Physics

The Appendix lists out all the values used for the parameters in this project

We now use the Considerations and Assumptions in section 3 to state and define the equation of motion for the carrier particle. This section will consider the main forces that are generally used to model the drug delivery of MNPs. Where we define the Carrier particles path taken in 3-D space as $\boldsymbol{r}(t) = x(t)\boldsymbol{e}_x + y(t)\boldsymbol{e}_y + z(t)\boldsymbol{e}_z$. The following forces acting on the carrier particle are:

1. The Magnetic Force $\boldsymbol{F}_m$ for a MNP is given by Lorentz Law [10]- MDD tumour growth]
$$\boldsymbol{F}_m = (\boldsymbol{m}\cdot\nabla)\boldsymbol{B} = \frac{2\pi r_{cp}}{3}\frac{X_p\mu_o}{1+\frac{X_p}{3}}\nabla(|\boldsymbol{B}|^2) = \frac{2\pi r_{cp}}{3}\frac{X_p\mu_o}{1+\frac{X_p}{3}}B\frac{\partial B}{\partial y}\boldsymbol{e}_y \tag{6}$$
The result involves assuming that our carrier particle is a sphere and assuming the magnetic force acts in only one direction and is of constant gradient. Here, $\boldsymbol{B}$ represents the magnetic field, r_{cp} the radius of the carrier particle, and μ_0 the magnetic susceptibility of free space. X_p represents the magnetic susceptibility of the particle.$B\frac{\partial B}{\partial y}$ represents the required magnetic gradient.We represent $\frac{X_p}{1+\frac{X_p}{3}} = \zeta$ a dimensionless number relating X_p. In this project, we approximate γ to be three.[3]

2. The Stokes Drag F_d. We again use the assumption that the carrier particle is a sphere, the vessel is large enough to experience posuielle flow (for $y \in (0, h]$) it suffices that
$$\boldsymbol{F}_d = -6\pi\mu r_{cp}(v_{cp} - v_f) = -6\pi\mu r_{cp}(\dot{x} - \frac{6U_0}{h^2}y(h-y))\boldsymbol{e}_x \tag{7}$$
Here, we have v_{cp} is the velocity of the carrier particle, v_f is the velocity of the fluid, μ_f is the viscosity of the fluid in the vessel and $\dot{x}$ represents $\frac{dx}{dt}$.

3. The Buoyancy force $\boldsymbol{F}_b$ can be applied for a large blood vessel (with diameter more than $1000\mu m$) [10] The buoyant force plays a role with the convective term due ti the mass if the Carrier particle. The buoyant force is given as
$$\boldsymbol{F}_b = -\frac{4\pi r_{cp}^3}{3}(\rho_{cp} - \rho_f)g\boldsymbol{e}_x \tag{8}$$

Where g represents the gravitational acceleration , ρ_{cp}, ρ_f represents the densities of the carrier particle and the fluid respectively.

4. The Saffman lift force can be applied for small particles in the shear field [10] Given that, we are using particles that are of nanosizes. The particles will experience a lift force perpendicular to the direction of flow - this force experienced is the Saffman Lift Force. The shear lift comes from the inertia effect in the viscous flow around the particle [10] The force is defined as:

$$\boldsymbol{F}_s = 8k'\mu\sqrt{\dot{\gamma}/\nu}r_{cp}^2(v_f - v_{cp}) \tag{9}$$

where $\dot{\gamma}$ is the shear rate of the fluid and k' is the shape factor,

By applying Newton's second law of motion we have that the sum of all forces must be equal to the mass multiplied by acceleration. Hence, the equation of motion becomes:

$$m_{cp}\frac{d^2\boldsymbol{r}}{dt^2} = \boldsymbol{F}_m + \boldsymbol{F}_d + \boldsymbol{F}_b + \boldsymbol{F}_s \tag{10}$$

5 Constructing A Model

The Appendix lists out all the values used for the parameters in this project

We now have the ingredients to construct a model showing the way a MNP moves in a blood vessel. In this model, we will consider the magnetic force and the drag force applied to the particle. Hence, this reduces equation 18 to $m_{cp}\frac{d^2\boldsymbol{r}}{dt^2} = \boldsymbol{F}_m + \boldsymbol{F}_d$ and provides us with the following system of equations

$$\frac{4\rho_{cp}\pi r_{cp}^3}{3}\begin{pmatrix}\ddot{x}\\ \ddot{y}\\ \ddot{z}\end{pmatrix} = \begin{pmatrix}0\\ \frac{2\pi r_{cp}}{3}\zeta B\frac{\partial B}{\partial y}\\ 0\end{pmatrix} - 6\pi\mu r_{cp}\begin{pmatrix}\dot{x} - \frac{6U_0}{h^2}y(h-y)\\ \dot{y}\\ \dot{z}\end{pmatrix}. \tag{11}$$

We make a substitution in 11, as we let $F^* = \frac{2\pi r_{cp}}{3}\zeta B\frac{\partial B}{\partial y}$ and drop the $\boldsymbol{e}_z$ component as our model will be based in two dimensions. We then non-dimensionalise these equations via the following relations:

$$XL = x \qquad Yh = y \qquad \tau T = t \qquad \tilde{x}L = x \qquad \tilde{y}L = y \tag{12}$$

This gives us the following system of equations:

$$M\frac{d^2X}{d\tau^2} = -\frac{dX}{d\tau} + 6Y(1-Y) \qquad \text{and} \qquad M\frac{d^2Y}{d\tau^2} = -\frac{dY}{d\tau} - N \tag{13}$$

Where dimensionless parameters M ans N are defined as

$$M = \frac{4\rho_{cp}r_{cp}^2U_0}{18\mu L} \qquad N = \frac{F^*L}{6U_0\pi\mu r_{cp}h}, \tag{14}$$

In this model we assume that the inertia force is negligible if $M << 1$ and that the diameter of the vessel is very small hence the left hand side of each equation in13 is negligible this reduces the equations to:

$$\frac{dX}{d\tau} = 6Y(1-Y) \qquad \text{and} \qquad \frac{dY}{d\tau} = -N \tag{15}$$

We now have a non-linear autonomous differential equations system - where our system does not explicitly depend on the independent variable τ. We will now apply analytical and numerical methods to studying the trajectories of the MNPs.

5.1 Analytical Approach to Solving the Model

The Appendix lists out all the values used for the parameters in this project

5.1.1 The Phase Plane Method

We now use the phase plane method to solve the system of equations. Given that $-N$ is a constant, we find that $Y(\tau) = Y$ will be a linear relationship between the parameter τ and output Y. Computing the nullclines we find that, $\frac{dY}{dX} = -\frac{-N}{6Y(1-Y)}$, with the nullclines not defined at $Y = 0$ or $Y = 1$. The stationary points occur at the point where the curve crosses the horizontal lines $Y = 0$ ans $Y = 1$. When calculating the eigenvalues at the points $A : (X_{cp0}, 0)$ and $B : (X_{cp1}, 1)$, we find that both have a singular eigenvalue of zero and a generalised eigenvector of $(1, 0)$. We do not have much information to understand the local behaviour, so we must solve them simultaneously to understand the relationship between the parameter τ and the way the curves move.

Hence, we arrive at the relations:

$$Y = -N\tau + c_1 \qquad X = -2N^2\tau^3 + 3N\tau^2(1 + 12c_1) + 6\tau(c_1 + c_!^2) + c_2, \tag{16}$$

where c_1 and c_2 are constants provided by boundary conditions. If we study the behavior of X and Y by taking the limit of τ, we see that X and Y become increasingly negative as $\tau \to \infty$. Hence the curves produced by the parameters will concentrate downwards as expected - because the particles will fall towards the target site . The curve representing the trajectory of the particle in terms of X and Y is given as

$$X(Y) = -2N^2\left(\frac{Y - c_1}{-N}\right)^3 + 3N\left(\frac{Y - c_1}{-N}\right)^2(1 + 12c_1) + 6\left(\frac{Y - c_1}{-N}\right)(c_1 + c_!^2) + c_2 \tag{17}$$

6 Results and Discussion

Figure 2 (left) shows the trajectories of the carrier particles under a magnetic field. In this case, we model it for a vein with an radius $r_{cp} = 10^{-6}m$. From the figure, we can see that the bottom plate where $Y = 0$ acts like a sink for the trajectories because as the particle moves up the vessel's length, eventually, the particle's path will converge towards the Y-axis. Hence, the magnetic field influences the particles as they are pulled towards the vessel wall. As the magnitude of the velocity of the blood is lower at the edges of the vessel, the horizontal component of the carrier's particle velocity decreases the closer to the vessel wall it gets.

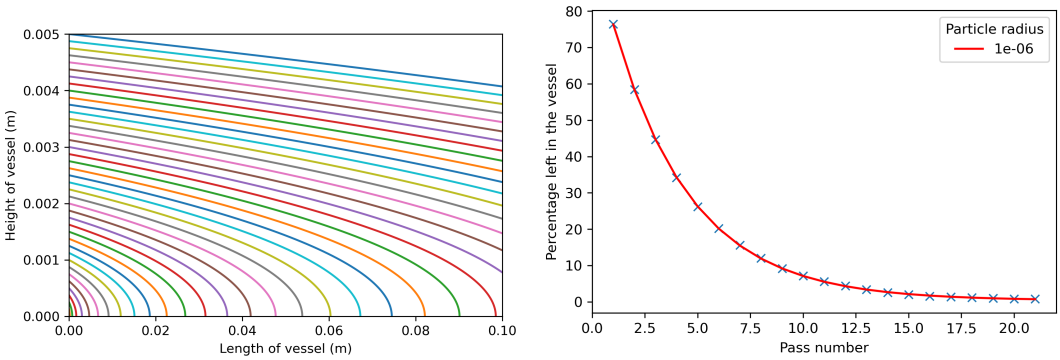

Figure 2: Trajectories of 40 particles in a vein with radius of the particle $r_{cp} = 10^{-6}m$ (left) and, The percentage of particles left in an artery with radius of the particle $r_{cp} = 10^{-6}m$ after each pass. The equation of best fit is given by: $99.395e^{0.269x} + 0.384$ (right).

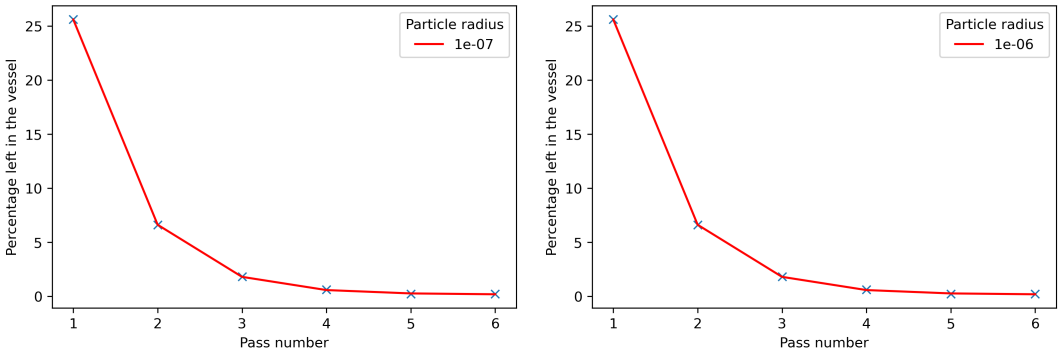

Figure 3: The percentage of particles left in artery with radius of particle $r_{cp} = 10^{-7}m$ after each pass. The equation of best fit is given by: $100.297e^{1.372x} + 0.152$ (left) and, The percentage of particles left in arteriole with radius of particle $r_{cp} = 10^{-6}$ after each pass. The equation of best fit is given by:$100.297e^{(1.372x)} + 0.152$. (right)

Figures 2 (left) and 3 (left) shows the results detailing the percentage of particles that enter the vessel reach the target area for two particles with radii $r_a = 10^{-6}m$ and $r_b = 10^{-7}m$ respectively. We can see a relationship between the radius of the carrier particle and the number of particles captured. The greater the particle radius,, the more particles are left after each pass,. Therefore, the number of passes required to meet the maximum number of particles to reach the vessel wall increases. The reason for this is that we see that the radius of the carrier particle has an inversely proportional relationship with the magnetic force. Hence, as the radius increases, the force applied to the particles due to the magnetic field decreases. Furthermore, this means that medics and engineers who design and deliver the process of Magnetic Drug Delivery need to consider the size of the carrier particle as we want the process to be as cost-effective as possible. As we have mentioned, the Drug Delivery process is expensive, and we would not like to have to waste resources on a patient.

We find that about 90% managed to be deposited in the target area by the ninth cycle with the arteriole. The carrier particles with radius $r = 10^{-6}m$ (seen in 3 (right)). The

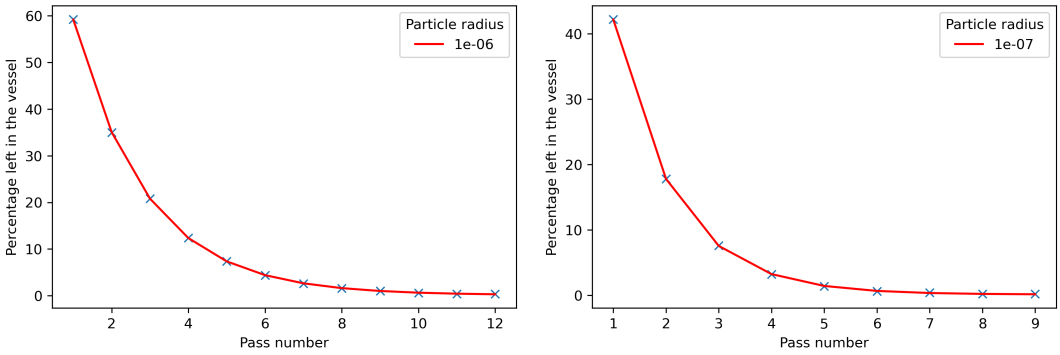

Figure 4: Percentage of particles left in Venule after each pass ;radius of particle: $r_{cp} = 10^{-6}$. The equation of best fit is given by: $99.821e^{0.525x} + 0.120$.(left) and, Percentage of particles left in Vein after each pass ; radius of particle: $r_{cp} = 10^{-6}$. The equation of best fit is given by: $99.591e^{0.203x} + 0.630$.(right)

figure shows a similar occurrence in comparison to how we tested the artery with $r = 10^{-7}m$. When we tested the arteriole with $r = 10^{-7}m$, all of the particles were deposited within a single cycle. The likely cause of this is the thinness of the blood vessel and the how slow the blood diffuses through the vessel's membrane. [2] Therefore, there is a large amount of time for the particles to diffuse at the target area of the vessel wall. Again, we see that the carrier particles with larger radii require more cycles due to the inverse relationship between the radius and the magnetic force.

In addition, we find that when passing through the venule, the particle all reach the wall after very few runs with $r = 10^{-6}m$. Where $r = 10^{-7}m$, all carrier particles reach the vessel wall after one cycle. As shown in 4 (left), we see that just like the arteriole the thinness of the vessel plays a part in how the many particles are captured per pass. Figure 4 (right) details the results for carrier particles in a vein where we have a similar result in comparison to the artery vessel.

From these results, we can conclude that having a carrier particle of radius $r_{cp} = 10^{-7}$ is more cost-effective as it is able to reach the target region more quickly and effectively in numbers. The results show that it deposited all the drug particles at the vessel wall in the fewest number of cycles for all vessels. We also find that magnetic drug delivery is most effective for smaller blood vessels as it takes fewer cycles to reach the maximum amount.

7 Limitations of the Model

With the provided resources, we've managed to conduct a mathematical representation model that shows hopes to realistically represent the process of magnetic drug delivery. The problem is that the model does have some limitations, and this mainly comes from the assumptions and considerations we've made previously. First, we said we assumed the cross-section of the blood vessel to be a perfect cylinder and that the fluid and the magnetic particles are

the only ones that flow down the bloodstream. This is a fault of the model because we do not consider the possible geometries of the blood vessels. There could be cases where the blood vessel may contain objects such as plaques which cause arteries to become clogged. In reality, the distribution of plaque is not even and symmetric hence this can alter the flow the blood undergoes. We didn't consider what happens when the width of the blood vessel is under $10\mu m$ (i.e. where poisuelle flow becomes invalid; hence the model breaks down). Another limitation is that the model does not factor in the possibility for the particle to have collisions with other particles in the bloodstream. In the real world, there will be other objects such as red blood cells and white blood cells in the bloodstream and the particle mould be guaranteed to collide with the other particles; hence if we assume that the particles have an inelastic collision, the particle will lose energy, and that will alter the behaviour of the particle. In addition, we find that not considering the Saffman lift force and Bouyancey force does not help to realistically represent the Magnetic Drug Delivery mathematically. We need the Saffman Lift Force for small particles with a shear field, and the buoyancy can be best represented for blood vessels that have diameters above $1000\mu m$.[10]

8 Conclusion

The project aimed to find the most mathematically accurate way to represent the process of Magnetic Drug Delivery. We have considered the process and what can be inferred from the critical aspects of the process. Then, we evaluated the assumptions and considerations that should be used in the project, Where we stated how the magnetic force will be of constant gradient and will act in only one direction. We then looked at the forces involved in Magnetic Drug Delivery and formulated a model using the forces we thought were simple and reasonable to use. The result is that we find that the path trajectories that a carrier particle will take will converge towards the vessel wall where the magnet is placed on top. We also find that the conditions most optimised are conditions where the vessel's size is smaller compared to larger vessels, and the carrier particles with smaller radii were most effective at getting the job done. Although, we have discussed the limitations of the model at length. We believe that the model can accurately represent the process as the other forces are defined as constant values. Hence, the effect of the additional forces would be more of a shift. We recommend a future avenue of research to look more into the additional forces and study various geometric aspects of blood vessels and see how things change on a case-by-case basis. In our situation, we have gone for the simplest case. We assumed the blood vessel was 100% pure the most relatable case for that is the healthiest human being alive being given the Magnetic Drug Delivery treatment, which is unlikely. We recommend the following sources as a guide to understanding the subject area. [5] [8] [12] [11] [10] [7]

$$m_{cp}\frac{d^2\boldsymbol{r}}{dt^2} = \boldsymbol{F}_m + \boldsymbol{F}_d + \boldsymbol{F}_b + \boldsymbol{F}_s \tag{18}$$

References

[1] S. Arshadi and A.R. Pishevar. Magnetic drug delivery effects on tumor growth, n.d.

[2] J.z Biasetti. Physics of blood flow in arteries and its relation to intra-luminal thrombus and atherosclerosis, n.d.

[3] Andrew D. Grief and Giles Richardson. Mathematical modelling of magnetically targeted drug delivery. *Journal of Magnetism and Magnetic Materials*, 293(1):455–463, 2005. Proceedings of the Fifth International Conference on Scientific and Clinical Apllications of Magnetic Carriers.

[4] Ian. Hawke. *MATH3018 MATH6141 Numerical Methods*. University of Southampton, 2017.

[5] Sam Howison. *Practical applied mathematics: modelling, analysis, approximation*. Cambridge university press, 2005.

[6] E. kianfar. Magnetic nanoparticles in targeted drug delivery: a review. journal of superconductivity and novel magnetism, 2021.

[7] Miguel Alfonso Mendez. Notes on 2d pulsatile poiseuille flows: An introduction to eigenfunction expansion and complex variables using matlab [image], 2016.

[8] Quentin Pankhurst, Stephen Jones, and Jon Dobson. Applications of magnetic nanoparticles in biomedicine. *Journal of Physics D: Applied Physics*, 49(50):501002, 2016.

[9] Giles Richardson. Math6149: Modelling with differential equations, 2022.

[10] S. Shaw, A. Sutradhar, and PVSN Murthy. Permeability and stress-jump effects on magnetic drug targeting in a permeable microvessel using darcy model. *Journal of Magnetism and Magnetic Materials*, 429:227–235, 2017.

[11] Sachin Shaw. Mathematical model on magnetic drug targeting in microvessel. In Neeraj Panwar, editor, *Magnetism and Magnetic Materials*, chapter 5. IntechOpen, Rijeka, 2018.

[12] Sibylle Sievers, Kai-Felix Braun, Dietmar Eberbeck, Stefan Gustafsson, Eva Olsson, Hans Werner Schumacher, and Uwe Siegner. Quantitative measurement of the magnetic moment of individual magnetic nanoparticles by magnetic force microscopy. *Small*, 8(17):2675–2679, 2012.

Blood Vessel Type	Diameter [m]	Length [m]	U_0 [ms^{-1}]
Artery	3 x 10^{-3}	1 x 10^{-1}	1 x 10^{-1}
Arteriole	3 x 10^{-5}	7 x 10^{-4}	1 x 10^{-2}
Venule	4 x 10^{-5}	8 x 10^{-4}	4 x 10^{-3}
Vein	5 x 10^{-3}	1 x 10^{-1}	1 x 10^{-1}

Table 1: A table showing the type of blood vessel and their corresponding diameter, length and velocity of the blood plasma going through them. This project has tested the performance of the model in each type of blood vessel with nanoparticles of two different radii.[3]

Parameter	Value
$\|\boldsymbol{B}\|$ the magnitude of the magnetic field	10^{-4}-1 $NAmp^{-1}m^{-1}$
μ_0 the density of the particle	$4\pi \times 10^{-7}$ $Amp^{-2}N$
μ the magnetic susceptibility of free space	$10^{-3}kgm^{-1}s^{-1}$
β the shape dependant magnetic susceptibility of the particle	3
ρ_{cp} the density of the particle	10^3-10^4 kgm^{-3}
ρ_b the density of blood	$1100kgm^{-3}$

Table 2: A table showing the values of typical measurements used in the study of magnetic drug delivery that have not been mentioned.[3]

9 Appendix

9.1 Declarations

- Analytical derivations and equations obtained by James Ashley, Delice Mambi-Lambu and Alex Pateman.
- Literature and parameter research conducted by Tsvetomira Pamukchieva, Delice Mambi-Lambu and Alex Pateman.
- Coding conducted by Jacinta Clovis, Aakash Datta, Matthew McCarthy and James Ashley.
- Graphical plots were provided by Aakash Datta and Matthew McCarthy.